Exploring dynamic light scattering microscopy (MicroDLS): a study of key parameters

Urquidi Gandarillas, Oscar; Brazard, Johanna; Adachi, Takuji

How to cite

URQUIDI GANDARILLAS, Oscar, BRAZARD, Johanna, ADACHI, Takuji. Exploring dynamic light scattering microscopy (MicroDLS): a study of key parameters. In: Proceedings Volume 12672, Applied Optical Metrology V. San Diego, United States. [s.l.] : SPIE, 2023. p. 8. (Proceedings) doi: 10.1117/12.2677534

This publication URL: https://archive-ouverte.unige.ch/unige:181115
Publication DOI: 10.1117/12.2677534

Exploring dynamic light scattering microscopy (MicroDLS): A Study of Key Parameters

Oscar Urquidi*, Johanna Brazard, Takuji B. M. Adachi*
Department of Physical Chemistry, Sciences II, University of Geneva, 30, Quai Ernest Ansermet, 1211 Geneva, Switzerland

*oscar.urquidigandarillas@unige.ch, takuji.adachi@unige.ch

ABSTRACT

Dynamic light scattering (DLS) is a technique used to characterize the size of nanometer and sub-micrometer particles in colloidal suspensions. Its non-destructive nature and simple usage make DLS widely applied in fundamental research, research and development (R&D), and quality control processes. While it is not uncommon to encounter the need to measure highly concentrated samples, the applicability of DLS is normally constrained by multiple sample and setup-dependent factors. MicroDLS, an optical microscope-based DLS design, has emerged as an effective alternative to measure highly concentrated or heterogeneous samples. Based on microDLS as a platform, we have been developing a method to improve the time resolution of measurements to further apply DLS to time-evolving systems. Herein, we performed various explorations of parameters to test the practical limit of applications by microDLS. Our setup is built based on a confocal optical microscope, a 532nm CW laser, a time-correlated single photon counting system, and a custom post-processing data analysis methodology. We explored the effects of the type of microscope objective and sample concentration in the measurement quality. The measurement of 60nm and 220nm polystyrene particles in suspension at different concentrations, showed the existence of an optimum working concentration range. Finally, the contrast between microscope objectives (20x NA0.4 and 4x NA0.1 air) revealed the specific technical challenges and limitations for each case.

Keywords: Dynamic light scattering, DLS, microDLS, particle size characterization

1. INTRODUCTION

Dynamic light scattering, or DLS, is a nondestructive optical technique for particle size metrology of colloids. DLS is extensively utilized in basic research[1] and industrial applications[2] for the characterization of sub-micrometer colloidal particles. Its working principle relies on the correlation of light intensity fluctuations over time, which arise by the interference of wavefronts scattered by individual colloidal particles under Brownian motion[3]. Particle size can generally be calculated from the diffusion coefficient, which in turn is obtained by fitting a physical model to the obtained correlation function.

DLS microscopy (micro-DLS), was conceived as an alternative method for performing DLS measurements where conventional systems often fail short. With its high spatial resolution, it can be used to investigate the size distribution of opaque solutions and the local properties in heterogeneous samples[4–6]. Among the various micro-DLS designs[4,7,8], the system proposed by Hiroi et al.[5] can be highlighted for it's simplicity and versatility. Recently, we developed a methodology to improve the time resolution of micro-DLS by several orders of magnitude compared with conventional DLS devices[9]. The improvement of the time-resolution may potentially broaden the application of DLS to study temporally evolving systems in a wide range of scientific and industrial research.

While the number of available designs for micro-DLS remains limited, the importance of its versatility in various conditions has been explored. Micro-DLS handles small probing volumes, at the femtoliter scale, and previous studies have highlighted that low particle concentration could potentially present a limitation[4]. There should be a concentration range that put the measurement condition out of the Gaussian process regime and the underlying theoretical framework is no longer applicable[10]. Furthermore, the selection of the objective lens impacts the mechanical configuration of the system, including the working distance, and the probing volume. This, in turn, significantly alters the contribution of detected signal components, and therefore affects the quality of the resulting reconstructed particle size distribution. The

study of these factors becomes even more relevant when dealing with time resolved measurements with short time windows, containing a limited number of correlated events.

2. MATERIALS AND METHODS

2.1 Setup Description

The micro-DLS setup was built on a confocal microscope configuration, based on the design of Hiroi *et al.*[5]. As it is depicted by figure 1, light from a 532nm laser (Laser Quantum, Opus 532) is coupled to a microscope objective (Olympus, 20x-NA0.4-air and 4x-NA0.1-air) by a telescope so it can be efficiently focused on the sample. The scattered light is then collected by the same objective and sent to the detection arm through a dichroic mirror (AHF, F73-512 Short pass Dichroic), where confocality is reached by placing a pinhole after the tube lens. Finally, the light is sent towards the detector (APD, Laser components GmbH, Count® Blue), through a relay lens (Thorlabs, 75 mm biconvex, LB4330), after passing through a 532nm bandpass filter (AHF, F94-532 HC laser clean-up maxline) and a neutral density filter (Thorlabs, ND10A). Detection is based on a time correlated single photon counting scheme, where a data acquisition module (PicoQuant, MultiHarp-150) detects single photons arriving at the detector, and each event is time tagged with a base reference sync signal of 80MHz. Data is sent to a computer and stored as a list of arrival times for post processing.

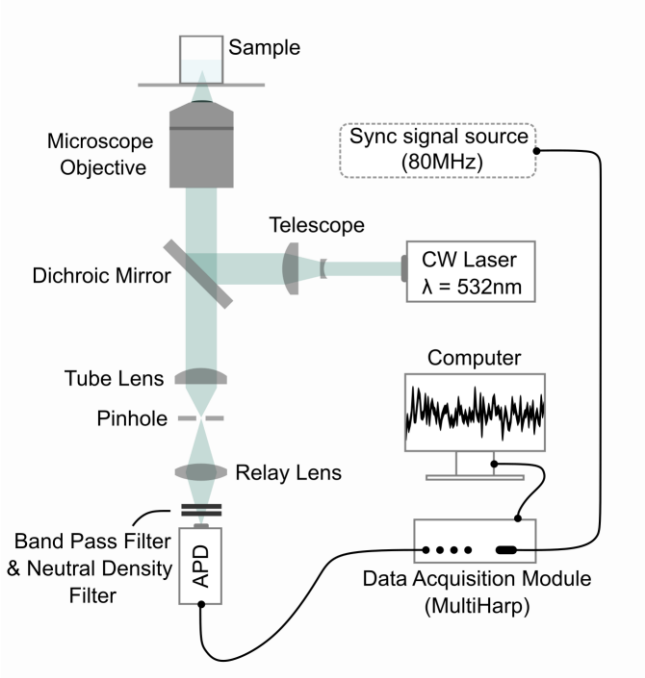

Figure 1. Schematic representation of the micro-DLS setup used in our study.

For the specific case of this micro-DLS design with a backscattering configuration (θ = 180˚), a heterodyne condition must be considered. As described by Hiroi *et al.*[5], for this geometry the detected signal is a combination of scattered light, from both single and multiple scattering, and a non-fluctuating signal coming from the direct reflection of the incoming beam at the glass interface. As already described in the literature, a DLS measurement under this heterodyne condition would generate an autocorrelation function (ACF) with a decay time systematically shifted from what its considered a correct value, and would require a correction to obtain an accurate measure of the particle size.

2.2 Acquisition and Postprocessing

The details of the acquisition and postprocessing used in this study were described in a previous work[9]. After acquisition, the stored photon arrival times were fed into a correlation algorithm, developed by Laurence *et al.*[11] to calculate an autocorrelation function (ACF) with a lag time binning strategy of progressively decreasing bin sizes. Later the particle size distribution was calculated from the autocorrelation by applying an inversion algorithm, solved numerically by non-

negative least squares optimization. Finally the particle size distribution was corrected for the effect of the non-fluctuating signal, by the so-called partial heterodyne treatment[5], which corrects the diffusion coefficient according to the autocorrelation amplitude. As mentioned before, this last step is crucial, because the main factor contributing to the loss of ACF amplitude is the reflected (non-fluctuating) signal reaching the detector.

3. EFFECT OF REFLECTED WAVEFRONT INTERFERENCE

While performing different measurements, we noticed a change in the photon count rate and ACF amplitude as we adjusted the position of the sample along the microscope sample holder plate. To illustrate this effect, we measured an aqueous suspension with 60 nm polystyrene beads at 0.1 wt%, with a 20x NA0.4 objective at a focal depth of 20 µm. Figure 2a-b show the concentric rings of the partially focused laser beam as it is reflected by the glass interface. A change of intensity in the central region can be observed as we slightly shift the sample along the sample holder plate (perpendicular to the optical axis). This behavior could be attributed to an effect of constructive (panel a) and destructive (panel b) interference of the reflected wavefront caused by mechanical shifts in the geometry. Most importantly, we observed that these two extreme conditions cause differences on the ACF amplitude. The ACF amplitude is about 0.3 (Figure 2c) at the condition shown in Figure 2b, which indicates that the non-fluctuating light component is considerably attenuated. On the other hand, the ACF amplitude decreases to ~0.07 at the position of Figure 2a. This effect should become significant, especially when samples with low scattering efficiency are measured or the measurement is performed very close to the glass interface. For our study, we chose to perform all measurements under the condition of maximum destructive interference (Figure 2b).

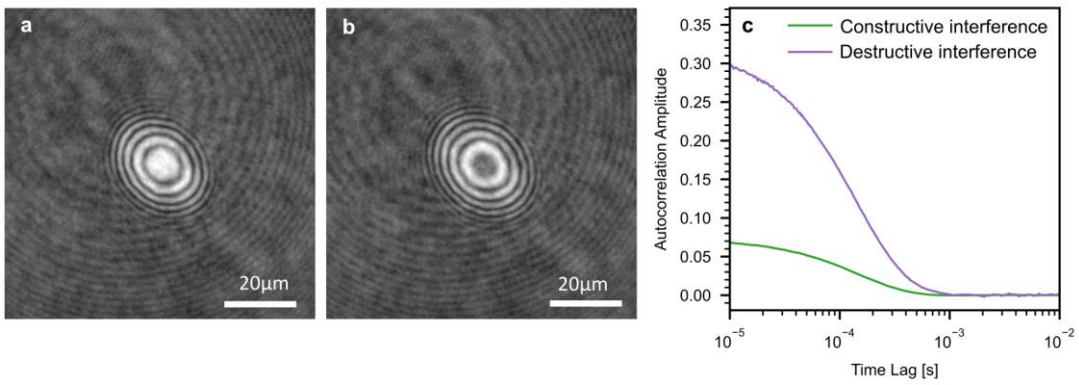

Figure 2. Effect of wavefront interference and how it changes depending on sample placement. Panels **a** and **b** show the microscope camera image illustrating the change of central intensity at different sample positions. Panel **c** shows the ACF at the two positions shown in the panel **a** and **b**.

4. EFFECT OF CONCENTRATION

60 nm and 220 nm polystyrene beads in water at different concentrations were used to study the effect of particle concentration on ACF. A 20x NA0.4 microscope objective and a pinhole size of 25 µm were used for all measurements. The laser power at the sample was adjusted between 250 µW and 7 mW, to maintain the photon count rate within the same order of magnitude for all measurements. The focal depth (from the glass-liquid interface) was also adjusted for each case to maintain a similar ACF amplitude. Each measurement was acquired for a total time of 30 s, and the ACF and size distributions were computed from the entire period.

Figure 3 shows the DLS measurements for different concentrations of 60 nm particles: 0.5, 0.1, 0.05, 0.01, $1x10^{-3}$, and $1x10^{-4}$ wt%. The ACFs computed for each concentration (Figure 3a) demonstrate how the amplitude varies with concentration. A distinctive change in amplitude can be observed at $1x10^{-3}$ wt%. Then the ACF at $1x10^{-4}$ wt% also shows apparent artifacts. From the scattering intensity transients (Figure 3 b1-6) we can qualitatively observe more isolated spikes at the lower concentrations. For the low concentration samples shown in the panels b5-6, the intensity transients show a slow change in the intensity. This can be explained as that the signal is dominated by the non-fluctuating reflection from the glass and the effect of slow mechanical displacements is clearly observed. This attribution

is well confirmed by the low ACF amplitude of the two lowest concentrations. The particle size (diameter) distribution function, calculated from the ACFs, shows small variance around the nominal particle diameter. As for the ACF and intensity timeseries, the size distribution for the least concentrated sample (panel c6) shows also a breaking point in quality, strongly deviating from the behavior of the other concentrations. From the result obtained for the range of sampled concentrations, we conclude that the fluctuation of the number of particles in the probing volume becomes a problem at $1x10^{-3}$ wt% but it is a severe issue at $1x10^{-4}$ wt% for 60 nm particles.

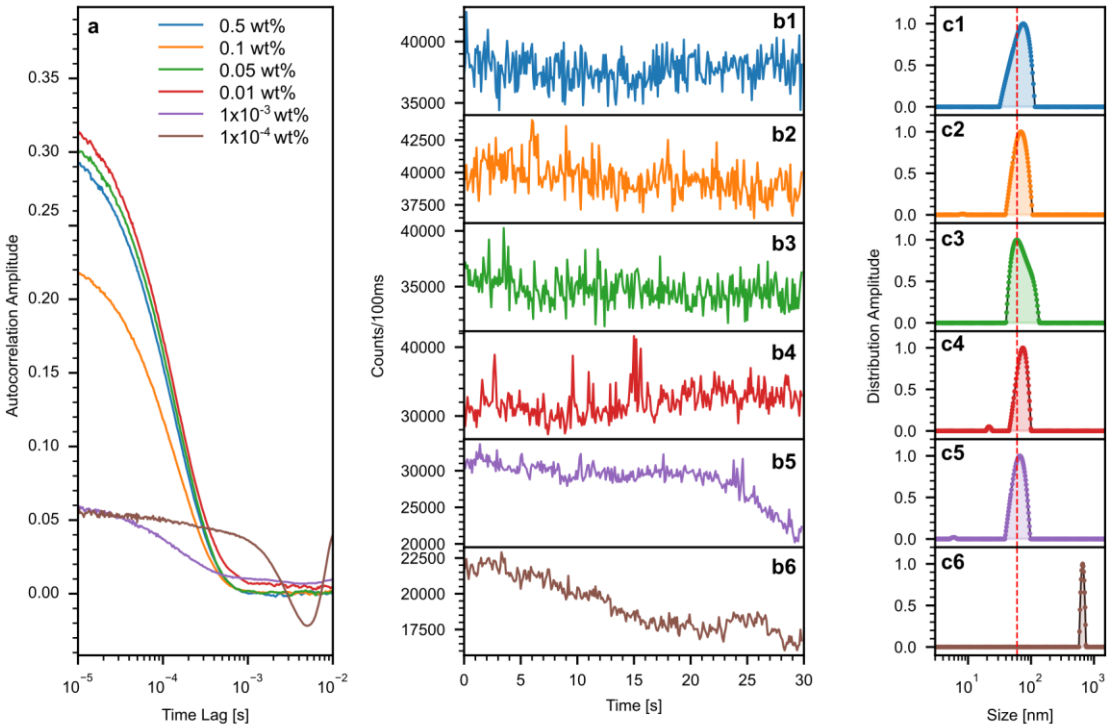

Figure 3. Effect of the change in concentration on the signal intensity time series, ACF and size distribution for 60nm particles. Panel a shows the ACF at different concentrations. Panels b1 – b6 show the signal intensity time series for different concentrations. Panels c1 – c6 show the reconstructed particle size for different concentrations, the red vertical line marks the nominal particle size of 60 nm.

Figure 4 shows the DLS measurements for different concentrations of 220 nm particles: 5, 1, 0.5, 0.1, 0.05, 0.01 and $1x10^{-3}$ wt%. The ACF amplitude (panel a) shows an overall decrease of the amplitude with a decrease in concentration, specially for the two concentrations (0.01 and $1x10^{-3}$ wt%) where an apparent artifact is also observed. Similar to the results on 60 nm particles, more isolated spikes appear on the intensity transients as concentration is decreased (Figure 4-b1 to b7). The particle size distribution of the measured samples show a main distribution component around the nominal value (220 nm) with some variations. The least concentrated samples (Figure 4-c6 and c7) show that the size distribution cannot be accurately constructed from the ACFs due to artifacts (Figure 4-b6 and b7). The mico-DLS measurement on 220 nm particles fail below the concentrations lower than 0.05 wt%. The lowest measurable concentration for 220 nm particles is higher than 60 nm particles. For a proper DLS measurement, the number of particles in a probing volume within the time bin used for constructing ACF must be steady. The number of particles at the same concentration in the unit of wt% for 60 nm is larger than 220 nm. Therefore, the artifacts are observed at a higher concentration for 220 nm.

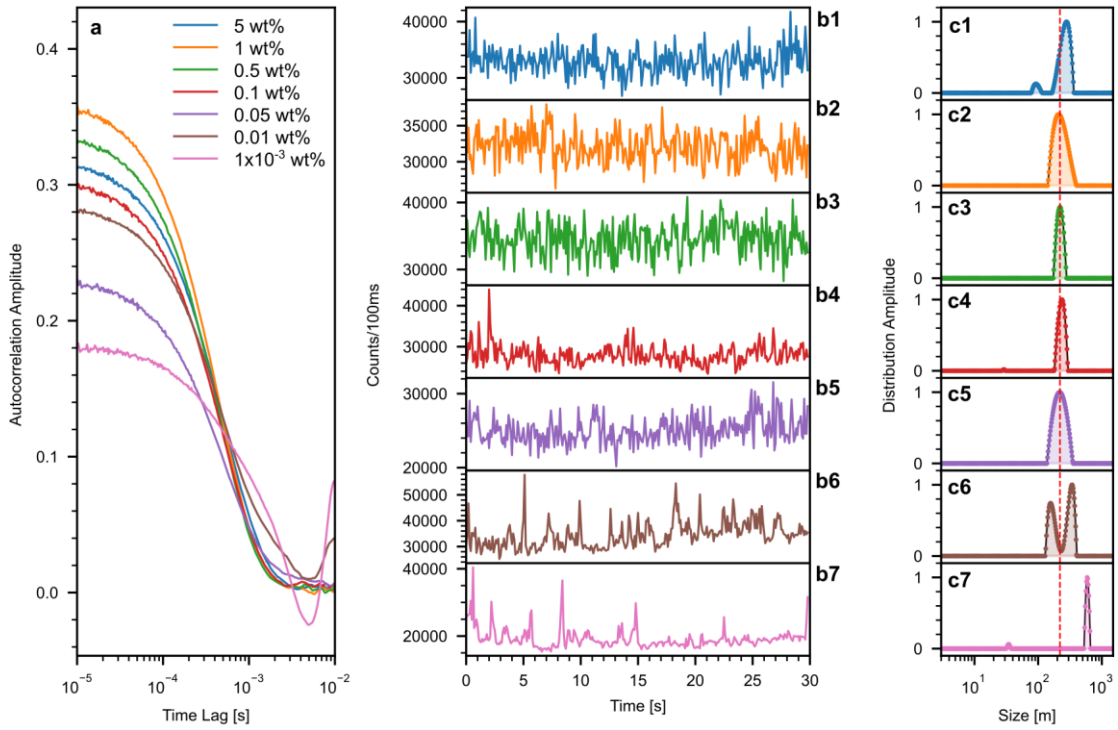

Figure 4. Effect of the change in concentration on the signal intensity time series, ACF and size distribution for 220nm particles. Panel a shows the ACF at different concentrations. Panels b1 – b7 show the signal intensity time series for different concentrations. Panels c1 – c7 show the reconstructed particle size for different concentrations, the red vertical line marks the nominal particle size of 220nm.

5. EFFECT OF OBJECTIVE AND SPATIAL FILTERING

One way to broaden the concentration range of the samples is to increase the probing volume. This could leverage the full potential of Micro-DLS across various applications and conditions. This could be achieved by choosing the right microscope objectives. This underscores the importance of investigating the implications of employing different objectives with distinctive properties, such as magnification and numerical aperture. For our study, we experimented with a 20X NA0.4-air objective and a 4X NA0.1-air objective. It's evident that this modification directly influences the size and shape of the confocal volume, which in turn significantly affects the amount of scattered light, both single and multiple scattering, as well as the reflected light from the glass interface. Moreover, this adjustment critically impacts the required degree of spatial filtering, which translates into the pinhole size used to reach confocality. In our study, we used pinholes of 25 µm and 50 µm for each objective, and performed measurements on an aqueous suspension of 60 nm polystyrene particles at 0.1 wt%. Measurements were taken at the same focal depth for each objective, 20 µm from the glass interface for 20X NA0.4 and 1.65 mm for 4X NA0.1. Laser power was adjusted to maintain the photon counts close to the same value (approximately $4x10^5$ counts/s)

As it is shown in figure 5a, the autocorrelation amplitude obtained for the 20x NA0.4 objective is consistently higher than for the 4x NA0.1 objective. This result was expected, since the lower magnification objective should have a larger confocal volume, accepting more light from the glass reflection resulting in the low ACF amplitude. The 4x NA 0.1 objective may also collect more multiple scattering, lowering the ACF amplitude. For both objectives, the use of a smaller pinhole size (25 µm, compared to 50 µm) resulted in an increase in the ACF amplitude. It is important to choose the pinhole size to reject the non-fluctuating light component and the multiple scattered light as much as possible. It becomes evident that the ACF amplitude shows a big contrast for the 20x NA0.4 objective when changing from 50 µm to 25 µm pinholes, resulting in similar size distributions close to the nominal value (panels b3 and b4). The 4x NA0.1

objective does not show a such a big contrast in amplitude by reducing the pinhole size, moreover the size distributions show a large deviation when moving from 50 µm to 25 µm pinhole sizes (panels b1 and b2). This could be attributed to the fact that even the 25 µm pinhole does not sufficiently reduce the non-fluctuating or multiple scattering components. The deviation is most likely caused by an overcorrection of the partial heterodyne treatment, where it is assumed that the main cause for the amplitude decrease is the non-fluctuating component. Probably for the 4x NA0.1 objective with 25 µm pinhole, the contribution of multiple scattering is not negligible.

It would be expected that the larger confocal volume of the lowest magnification objective could in principle enable the measurement of low concentration samples. In practice, our results suggest that under a confocal, backscattering (θ = 180˚) micro-DLS design, there would always exist a large enough non-fluctuating (reflected) light component, preventing the successful measurement of diluted samples. Moreover, a preliminary exploration suggested that the use of smaller pinhole sizes (5 or 2 µm) would decrease the autocorrelation quality further while requiring the use of much higher powers (up to 100 times higher) on the sample, where optical trapping could start to be an issue.

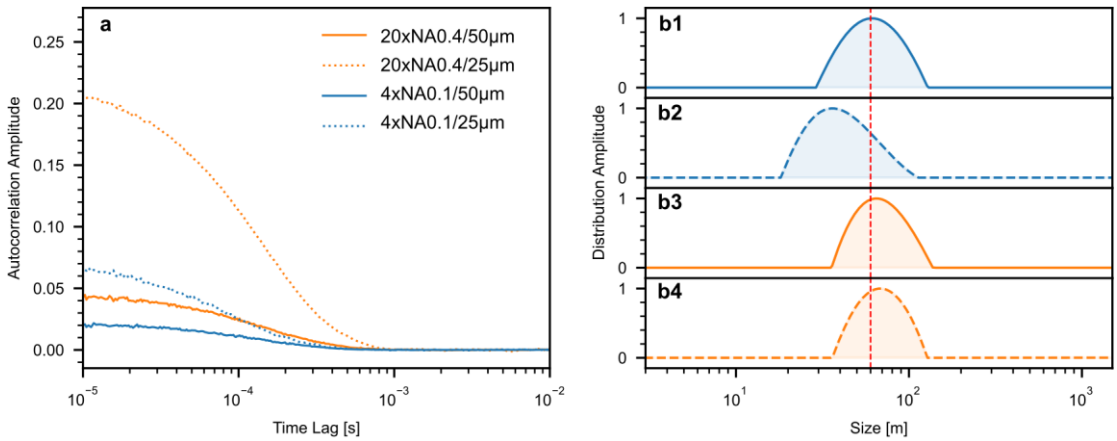

Figure ~~4~~5. Effect of the objective and pinhole size in ACF amplitude and size distribution for 60nm. Panel a shows the change in ACF with different objective-pinhole combinations. Panels b1 – b4 show the reconstructed particle size distributions with different objective-pinhole combinations, the red vertical line marks the nominal particle size of 60nm.

6. CONCLUSIONS

We explored how key parameters influence the capacity of micro-DLS to reconstruct particle size distributions. We found that the interference of reflected and incoming wavefronts, along with mechanical variations present on the sample container and supporting surfaces, induce conditions of both constructive and destructive interference. This interference in turn affects the intensity of the detected non-fluctuating signal component, and ultimately influences the ACF amplitude and decay rate, which can be used in our favor. Moreover, we demonstrated that particle concentration significantly impacts the quality of the ACF and the particle size distribution. Specifically, the quality of ACF and size distribution deteriorates at the concentrations lower than 0.01 wt% for 60 nm and 0.05 wt% for 220 nm particles. This is likely due to the large fluctuations in the number of particles within the probing volume. These findings underscore the need for careful consideration when determining minimum sample concentration where micro-DLS is generally more advantageous for highly concentrated samples. Our investigation was also extended to the use of microscope objectives of different numerical apertures and magnifications. Here, we established that a 20x NA0.4 objective outperforms the 4x NA0.1 objective in limiting the effect of multiple scattering and non-fluctuating light signal contributions, reaching higher ACF amplitudes and consistent size distributions. This final point accentuates the importance of carefully selecting an adequate pinhole-objective pair to ensure accurate size distribution measurements, while maintaining optimal detection efficiency.

REFERENCES

[1] Cao, A., "Light Scattering. Recent Applications," Analytical Letters **36**(15), 3185–3225 (2003).

[2] Hassan, P. A., Rana, S. and Verma, G., "Making Sense of Brownian Motion: Colloid Characterization by Dynamic Light Scattering," Langmuir **31**(1), 3–12 (2015).

[3] Pecora, R., ed., [Dynamic Light Scattering: Applications of Photon Correlation Spectroscopy], Springer US, Boston, MA (1985).

[4] Kaplan, P. D., Trappe, V. and Weitz, D. A., "Light-scattering microscope," Appl. Opt. **38**(19), 4151 (1999).

[5] Hiroi, T. and Shibayama, M., "Dynamic light scattering microscope: Accessing opaque samples with high spatial resolution," Opt. Express **21**(17), 20260 (2013).

[6] Hiroi, T. and Shibayama, M., "Measurement of Particle Size Distribution in Turbid Solutions by Dynamic Light Scattering Microscopy," JoVE(119), 54885 (2017).

[7] Wang, J.-C., "Design and testing of a novel microscopic photon correlation spectrometer with higher accuracy," J. Opt. A: Pure Appl. Opt. **3**(5), 360–365 (2001).

[8] Qiu, X.-L., Tong, P. and Ackerson, B. J., "Proposal and testing of dual-beam dynamic light scattering for two-particle microrheology," Appl. Opt. **43**(17), 3382 (2004).

[9] Urquidi, O., Barbosa, N., Brazard, J. and Adachi, T. B. M., "Toward time resolved dynamic light scattering microscopy: Retrieving particle size distributions at high temporal resolutions," Review of Scientific Instruments **94**(8), 083101 (2023).

[10] Lemieux, P.-A. and Durian, D. J., "Investigating non-Gaussian scattering processes by using nth -order intensity correlation functions," J. Opt. Soc. Am. A **16**(7), 1651 (1999).

[11] Laurence, T. A., Fore, S. and Huser, T., "Fast, flexible algorithm for calculating photon correlations," Opt. Lett. **31**(6), 829 (2006).